Article

Zeolite-Catalyzed Hydrogenation of Carbon Dioxide and Ethene

Bun Chan, and Leo Radom

J. Am. Chem. Soc., **2008**, 130 (30), 9790-9799 • DOI: 10.1021/ja800840q • Publication Date (Web): 01 July 2008

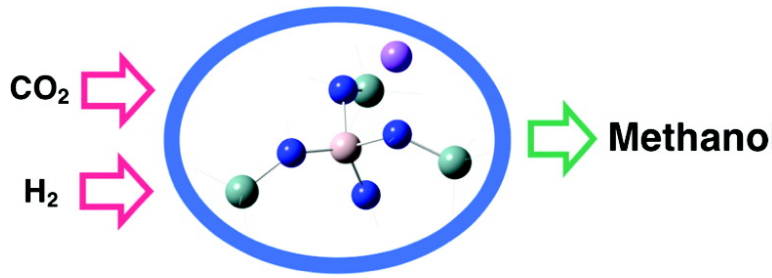

More About This Article

Additional resources and features associated with this article are available within the HTML version:

- Supporting Information
- Access to high resolution figures
- Links to articles and content related to this article
- Copyright permission to reproduce figures and/or text from this article

View the Full Text HTML

J|A|C|S
ARTICLES

Published on Web 07/01/2008

Zeolite-Catalyzed Hydrogenation of Carbon Dioxide and Ethene

Bun Chan* and Leo Radom*

School of Chemistry and Centre of Excellence for Free Radical Chemistry and Biotechnology, University of Sydney, Sydney, NSW 2006, Australia

Received February 2, 2008; E-mail: chan_b@chem.usyd.edu.au; radom@chem.usyd.edu.au

Abstract: Ab initio molecular orbital theory and density functional theory calculations have been used to study the three-stage zeolite-catalyzed hydrogenation of CO_2 to methanol and the hydrogenation of C_2H_4 to ethane, with the aim of designing an effective zeolite catalyst for these reactions. Both Brønsted acid (XH) and alkali metal (XM) sites in model zeolites (-X−Al−XH- or -X−Al−XM-) have been examined. It is found that appropriately designed zeolites can provide excellent catalysis for these reactions, particularly for the hydrogenation of CO_2, HCO_2H and CH_2O, with uncatalyzed barriers of more than 300 kJ mol^{-1} being reduced to as little as 17 kJ mol^{-1} (in the case of CH_2O). The reaction barrier depends on the acidity of the XH moiety or the nature of the metal cation M in the XM moiety, and the basicity of the adjacent X group in the catalyst. For a catalyst based on alkali metal zeolites (XM), the catalytic activity is relatively insensitive to the nature of X in the XM group. As a result, the catalytic activity for these types of zeolites increases as X becomes more basic. We propose that alkali metal zeolites with Ge and N incorporated into the framework could be very effective catalysts for hydrogenation processes.

1. Introduction

Carbon dioxide has been widely recognized as a potent greenhouse gas and is linked to the problem of global warming.[1] As a result, recycling of CO_2 has been a topic of intense research[2] and a subject of discussion not only from a scientific but also from an ecological−political point of view. Because CO_2 is a highly oxidized, thermodynamically stable compound, its utilization requires reaction with specific high-energy substances. Catalytic hydrogenation is one of the most promising approaches to CO_2 fixation.

Hydrogenation of CO_2 can lead to a variety of useful compounds such as methanol, hydrocarbons, esters, and ethers. Within this list, methanol holds a central position, as it is one of the key petrochemicals in industry. For instance, over 29 million metric tons of methanol were produced worldwide in 1994.[3] Industrially, methanol is produced catalytically from synthesis gas, which is a mixture of CO, CO_2, and H_2 in various proportions. The catalysts generally contain Cu and a mixture of oxides such as ZnO/Al_2O_3. More generally, most catalysts for hydrogenation reactions contain transition metals, both in chemical[4] and biological[5] systems.

In contrast to transition-metal-catalyzed hydrogenations, catalytic hydrogenation without transition metals has received much less attention. Among studies of transition-metal-free hydrogenation, it has been found that strong acids can be used as catalysts for the hydrogenation of unsaturated hydrocarbons.[6] It has also been observed that some carbonyl compounds undergo catalytic hydrogenation in the presence of a strong base.[6a,b,7] Furthermore, it has been demonstrated that zeolites catalyze the hydrogenation of alkenes.[8] Very recently, Stephan and co-workers reported the first metal-free catalytic hydrogenation under mild conditions using phosphonium borates.[9] There have also been several theoretical studies of hydrogenation reactions catalyzed by acids and bases.[10] Results from these studies have revealed a common feature for these reactions: the

(1) See, for example: (a) Hoffert, M. I. *Science* **2002**, *298*, 981. (b) Pacala, S.; Socolow, R. *Science* **2004**, *305*, 968. (c) Bauen, A. *J. Power Sources* **2006**, *157*, 893.

(2) For recent reviews, see: (a) Hashimoto, K.; Habazaki, H.; Yamasaki, M.; Meguro, S.; Sasaki, T.; Katagiri, H.; Matsui, T.; Fujimura, K.; Izumiya, K.; Kumagai, N.; Akiyama, E. *Mater. Sci. Eng., A* **2001**, *A304−306*, 88. (b) Song, C. *Catal. Today* **2006**, *115*, 2. (c) Aresta, M.; Dibenedetto, A. *Dalton Trans.* **2007**, 2975. (d) Sakakura, T.; Choi, J.-C.; Yasuda, H. *Chem. Rev.* **2007**, *107*, 2365.

(3) Farrauto, R. J.; Bartholomew, C. H. *Fundamentals of Industrial Catalytic Processes*, 2nd ed.; Wiley: New York, 2005.

(4) See, for example: (a) Jacobsen, E. N.; Pfaltz, A.; Yamamoto, H., Eds. *Comprehensive Asymmetric Catalysis*; Springer: Berlin, 1999; Vol. 1. (b) Nishimura, S. *Handbook of Heterogeneous Catalytic Hydrogenation for Organic Synthesis*; Wiley: New York, 2001. (c) Genet, J.-P. *Acc. Chem. Res.* **2003**, *36*, 908. (d) Wills, M. *Science* **2006**, *311*, 619.

(5) For general reviews on hydrogenases, see: (a) Albracht, S. P. J. *Biochim. Biophys. Acta* **1994**, *1188*, 167. (b) Cammack, R. *Nature* **1995**, *373*, 556. (c) Ermler, U.; Grabarse, W.; Shima, S.; Goubeaud, M.; Thauer, R. K. *Curr. Opin. Struct. Biol* **1998**, *8*, 749. (d) Evans, D. J.; Pickett, C. J. *Chem. Soc. Rev.* **2003**, *32*, 268. (e) Shima, S.; Thauer, R. K. *Chem. Rec.* **2007**, *7*, 37.

(6) (a) Walling, C.; Bollyky, L. *J. Am. Chem. Soc.* **1961**, *83*, 2968. (b) Walling, C.; Bollyky, L. *J. Am. Chem. Soc.* **1964**, *86*, 3750. (c) Siskin, M. *J. Am. Chem. Soc.* **1974**, *96*, 3641.

(7) Berkessel, A.; Schubert, T. J. S.; Müller, T. N. *J. Am. Chem. Soc.* **2002**, *124*, 8693.

(8) See, for example: (a) Sano, T.; Hagiwara, H.; Okabe, K.; Okado, H.; Saito, K.; Takaya, H. *Sekiyu Gakkaishi* **1986**, *29*, 89. (b) Bader, R. R.; Baumeister, P.; Blaser, H.-U. *Chimia* **1996**, *50*, 99. (c) Aboul-Gheit, A. K.; Aboul-Fotouh, S. M.; Abdel-Hamid, S. M.; Aboul-Gheit, N. A. K. *Appl. Catal., A* **2006**, *297*, 102.

(9) Chase, P. A.; Welch, G. C.; Jurca, T.; Stephan, D. W. *Angew. Chem., Int. Ed.* **2007**, *46*, 8050.

10.1021/ja800840q CCC: $40.75

catalyst operates in a bifunctional acid−base fashion to give rise to heterolytic cleavage of H_2 into effectively an H^+ plus an H^-.

Among transition-metal-free catalysts for hydrogenation, zeolites represent a particularly interesting class due to the existence of a large variety of natural/synthetic zeolites with a variety of acid/base properties.[11] Typically, zeolite catalysis involves acid-catalyzed reactions, with many industrial applications in petroleum refining, synfuels production, and petrochemical production. In addition, a number of base-catalyzed zeolite reactions have been reported.[12] Recently, several research groups have succeeded in synthesizing nitrogen-containing zeolites, with possibly enhanced basicity.[13] In addition, recent theoretical studies have demonstrated the importance of both basic as well as acidic sites in a zeolite for the heterolytic cleavage of the C−X bond in CH_3X.[14,15] These preliminary results further open up the possibility of combining the acidic and basic properties in a zeolite for bifunctional catalysis. Further enhancement in catalytic activity might be achieved by modifying the zeolite through replacement of the Si/Al atoms in the zeolite framework. For example, it has been shown that substitution of Si by Ge results in improved catalytic activity in both acid- and base-catalyzed reactions.[16]

As part of a continuing study,[10b–f,17,18] we have been interested in pursuing the fundamentals of transition-metal-free hydrogenation. In a preliminary communication in this journal,[17] we demonstrated that, with appropriate substitution of specific atoms in a zeolite, the resulting material can potentially be an effective catalyst for the complete hydrogenation of CO_2. In the present paper, we employ quantum chemistry computations to systematically extend our study on the zeolite-catalyzed, three-stage hydrogenation of CO_2 to methanol:

$$O=C=O + H_2 \rightarrow HO-CH=O \quad (a)$$

$$HO-CH=O + H_2 \rightarrow HO-CH_2-OH \rightarrow CH_2=O + H_2O \quad (b)$$

$$CH_2=O + H_2 \rightarrow CH_3-OH \quad (c)$$

We also probe the possibility of using a zeolite to catalyze the hydrogenation of nonpolar bonds, by examining the zeolite-catalyzed hydrogenation of C_2H_4, a prototypical nonpolar substrate:

$$H_2C=CH_2 + H_2 \rightarrow H_3C-CH_3 \quad (d)$$

Our goal is to obtain a better understanding of this subject, and consequently to be able to rationally design effective zeolite catalysts for hydrogenation.

2. Computational Details

Standard ab initio molecular orbital theory and density functional theory calculations[19] were carried out with the Gaussian 03[20] and MOLPRO 2002[21] programs. For small models of the zeolites (4T) and related complexes and transition structures, geometries were obtained at the B3-LYP/6−31+G(d,p) level of theory, while improved relative energies were obtained at the MP2/G3MP2Large[22] level. Benchmark calculations were also carried out at the G3(MP2)-RAD level.[23]

Structures involving larger zeolite models were obtained with a different approach. Models representing cavities of the MFI structure[24] were constructed by extracting a 28T-cluster from the literature crystal structure.[25] Si and O atoms in a selected 4T-portion within the 28T-cluster were substituted with atoms that correspond

(10) (a) Siria, J. C.; Duran, M.; Lledós, A.; Bertrán, J. *J. Am. Chem. Soc.* **1987**, *109*, 7623. (b) Scott, A. P.; Golding, B. T.; Radom, L. *New. J. Chem.* **1998**, 1171. (c) Senger, S.; Radom, L. *J. Phys. Chem. A* **2000**, *104*, 7375. (d) Senger, S.; Radom, L. *J. Am. Chem. Soc.* **2000**, *122*, 2613. (e) Chan, B.; Radom, L. *Aust. J. Chem.* **2004**, *57*, 659. (f) Chan, B.; Radom, L. *J. Am. Chem. Soc.* **2005**, *127*, 2443.

(11) For an overview of zeolites and their applications, see: (a) Weitkamp, J.; Puppe, L., Eds. *Catalysis and Zeolites: Fundamentals and Applications*; Springer: New York, 1999. (b) van Bekkum, H.; Flanigen, E. M.; Jansen, J. C., Eds. *Introduction to Zeolite Science and Practice*, 2nd ed.; Elsevier: New York, 2001. (c) Auerbach, S. M.; Carrado, K. A.; Dutta, P. K., Eds. *Handbook of Zeolite Science and Technology*; Dekker:New York, 2003. (d) Stoecker, M. *Microporous Mesoporous Mater.* **2005**, *82*, 257.

(12) See, for example:(a) Hathaway, P. E.;; Davis, M. E. J. *Catal* **1988**, *117*, 497. (b) Tsuji, H.; Yagi, F.; Hattori, H. *Chem. Lett.* **1991**, 1881. (c) Gortsema. ; F. P.; Beshty, B.; Friedman, J. J.; Matsumoto, D.; Sharkey, J. J.; Wildman, G.; Blacklock, T. J.; Pan, S. H. In *Catalysis of Organic Reactions (Chemical Industries)*; Kosak, J. R., ; Johnson, T. A. Eds.; Dekker: New York. 1993, Vol. 53. pp 445−>460. (d) Barthoomeuf, D. *Cat. Rev. - Sci. Eng.* **1996**, *38*, 521. (e) Davis, R. J. *J. Catal.* **2003**, *216*, 396. (f) Romero, M. D.; Ovejero, G.; Rodriguez, A.; Gomez, J. M. *Microporous Mesoporous Mater.* **2005**, *81*, 313.

(13) See, for example:(a) Ernst, S.; Hartmann, M.; Sauerbeck, S.; Bongers, T. *Appl. Catal. A: General* **2000**, *200*, 117. (b) Xia, Y.; Mokaya, R. *Angew. Chem., Int. Ed* **2003**, *42*, 2639. (c) Xiong, J.; Ding, Y.; Zhu, H.; Yan, L.; Liu, X.; Lin, L. *J. Phys. Chem. B* **2003**, *107*, 1366–1369. (d) Zhang, C.; Xu, Z.; Wan, K.; Liu, Q. *Appl. Catal. A* **2004**, *258*, 55. (e) Guo, J.; Han, A.-J.; Yu, H.; Dong, J.-P.; He, H.; Long, Y.-C. *Microporous Mesoporous Mater.* **2006**, *94*, 166.

(14) (a) Lesthaeghe, D.; Van Speybroeck, V.; Waroquier, M. *J. Am. Chem. Soc.* **2004**, *126*, 9162. (b) Lesthaeghe, D.; Van Speybroeck, V.; Marin, G. B.; Waroquier, M. *J. Phys. Chem. B* **2005**, *109*, 7952. (c) Hemelsoet, K.; Lesthaeghe, D.; Van Speybroeck, V.; Waroquier, M. *Chem. Phys. Lett.* **2006**, *419*, 10. (d) Hemelsoet, K.; Lesthaeghe, D.; Van Speybroeck, V.; Waroquier, M. *J. Phys. Chem. C* **2007**, *111*, 3028. (e) Zheng, A.; Wang, L.; Chen, L.; Yue, Y.; Ye, C.; Lu, X.; Deng, F. *ChemPhysChem* **2007**, *8*, 231.

(15) For other computational studies on zeolites, see for example: (a) Corma, A. *Curr. Opin. Solid State Mater. Sci.* **1997**, *2*, 63. (b) Bonn, M.; Bakker, H. J.; Domen, K.; Hirose, C.; Kleyn, A. W.; Van Santen, R. A. *Catal. Rev.-Sci. Eng.* **1998**, *40*, 127. (c) Sauer, J.; Sierka, M. *J. Comput. Chem.* **2000**, *21*, 1470. (d) Payne, M. C.; Hytha, M.; Stich, I.; Gale, J. D.; Terakurag, K. *Microporous Mesoporous Mater.* **2001**, *48*, 375. (e) Zygmunt, S. A.; Curtiss, L. A. In *Computational Materials Chemistry: Methods and Applications*; Curtiss, L. A., ; Gordon, M. S., Eds.; Kluwer Academic Publishers: Dordrecht, 2004; pp 191−245. (f) Mignon, P.;; Geerlings, R.;; Schoonheydt, R. *J. Phys. Chem. B* **2006**, *110*, 24947. (g) Mignon, P.; Geerlings, R.; Schoonheydt, R. *J. Phys. Chem. C* **2007**, *111*, 12376. (h) Pidko, E. A.; Hensen, E. J. M.; Van Santen, R. A. *J. Phys. Chem. C* **2007**, *111*, 13068.

(16) See for example: (a) Corma, A.; Martín-Aranda, R. M.; Sánchez, F. *J. Catal.* **1990**, *126*, 192. (b) Concepcion-Heydorn, P.; Jia, C.; Herein, D.; Pfander, N.; Karge, H. G.; Jentoft, F. C. *J. Mol. Catal. A* **2000**, *162*, 227. (c) van de Water, L. G. A.; van der Waal, J. C.; Jansen, J. C.; Maschmeyer, T. *J. Catal.* **2004**, *223*, 170.

(17) Chan, B.; Radom, L. *J. Am. Chem. Soc.* **2006**, *128*, 5322.

(18) (a) Zhong, G.; Chan, B.; Radom, L. *J. Am. Chem. Soc.* **2007**, *129*, 924. (b) Zhong, G.; Chan, B.; Radom, L. *THEOCHEM* **2007**, *811*, 13. (c) Chan, B.; Radom, L. *J. Phys. Chem. A* **2007**, *111*, 6456.

(19) See for example: (a) Hehre, W. J.; Radom, L.; Schleyer, P. v. P.; Pople, J. A. *Ab Initio Molecular Orbital Theory*; Wiley: New York, 1986. (b) Jensen, F. *Introduction to Computational Chemistry*, 2nd ed.; Wiley, Chichester, 2007. (c) Koch, W.; Holthausen, M. C. *A Chemist's Guide to Density Functional Theory*, 2nd ed.; Wiley: New York, 2001.

(20) Frisch, M. J., et al. Gaussian 03, Revision D.02; Gaussian, Inc, Wallingford CT, 2004.

(21) MOLPRO, 2002.6 is a package of ab initio programs written by H.-J. Werner et al.

(22) The G3MP2Large basis set is similar to the 6−311+G(3df,2p) basis set but employs 3d2f polarization functions on second-row elements and 2df polarization functions on first-row elements. See: (a) Curtiss, L. A.; Raghavachari, K.; Redfern, P. C.; Rassolov, V.; Pople, J. A. *J. Chem. Phys.* **1998**, *109*, 7764. (b) Curtiss, L. A.; Redfern, P. C.; Raghavachari, K.; Rassolov, V.; Pople, J. A. *J. Chem. Phys.* **1999**, *110*, 4703.

(23) (a) Henry, D. J.; Sullivan, M. B.; Radom, L. *J. Chem. Phys.* **2001**, *118*, 4849. (b) Henry, D. J.; Parkinson, C. J.; Mayer, P. M.; Radom, L. *J. Phys. Chem. A* **2001**, *105*, 6750. (c) Henry, D. J.; Sullivan, M. B.; Radom, L. *J. Chem. Phys.* **2003**, *118*, 4849.

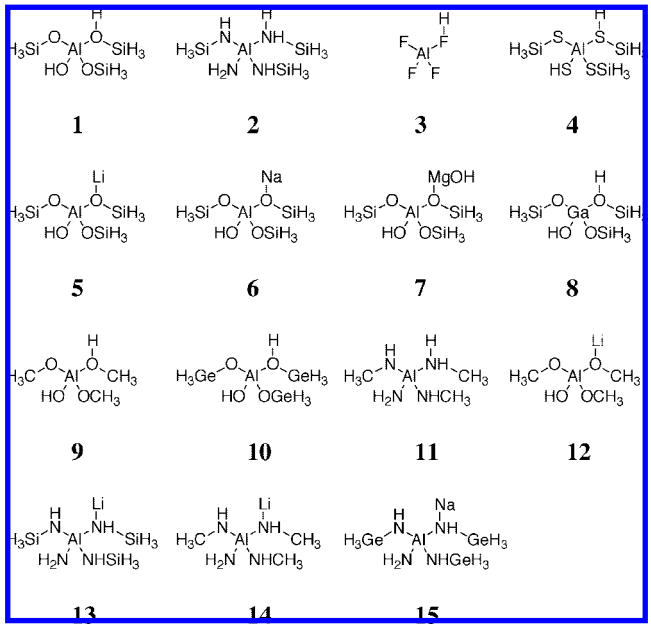

Figure 1. Model zeolites employed in this study.

to those in the 4T-clusters **1**, **2**, and **15** (see Figure 1 above). Dangling bonds were saturated with hydrogen atoms, whose locations were obtained through optimizations with the PM3 semiempirical procedure with the heavy atoms being frozen. In subsequent ONIOM[26] calculations, the clusters were partitioned into two layers, with atoms corresponding to those in the 4T-clusters belonging to the high-level layer. Geometry optimizations were carried out at the ONIOM(B3-LYP/6−31+G(d,p):PM3) level, where only the high-level atoms were optimized. Improved energies were obtained through calculations on these structures at the ONIOM(MP2/G3MP2Large:HF/6−31+G(d,p)) level. For complexes and transition structures, the substrates were also included in the high-level layer.

The intrinsic reaction coordinate (IRC) method was employed to confirm that each transition structure is linked to the appropriate adjacent minima. Unless otherwise noted, geometrical parameters for structures that involve 4T-clusters are B3-LYP/6−31+G(d,p) values. Relative energies correspond to MP2/G3MP2Large values at 0 K. For 28T-clusters and related structures, geometrical parameters refer to ONIOM(B3-LYP/6−31+G(d,p):PM3) values, while relative energies correspond to ONIOM(MP2/G3MP2Large:HF/6−31+G(d,p) values at 0 K. Zero-point vibrational energies (ZPVEs), derived from B3-LYP/6−31+G(d,p) (for 4T clusters) or ONIOM(B3-LYP/6−31+G(d,p):PM3) (for 28T clusters) frequencies, were incorporated into total energies. Literature scaling factors[27] were used in the evaluation of ZPVEs (0.9806) from the B3-LYP or ONIOM harmonic vibrational frequencies.

Table 1. Calculated Overall ($E^{\ddagger}_o$) and Central ($E^{\ddagger}_c$) Barriers (kJ mol^{-1}) and Reaction Enthalpies (ΔH) for Uncatalyzed and Catalyzed (by **1**) Hydrogenation Reactions

	uncatalyzed							
	$E^{\ddagger}_o$(a)	$E^{\ddagger}_o$(b)	$E^{\ddagger}_o$(c)	$E^{\ddagger}_o$(d)	ΔH(a)	ΔH(b)	ΔH(c)	ΔH(d)
MP2/G3MP2Large	323	327	301	365	40	−2	−81	−133
G3(MP2)-RAD	324	326	305	359	31	−2	−76	−121

	catalyzed by **1**							
	$E^{\ddagger}_o$(a)	$E^{\ddagger}_o$(b)	$E^{\ddagger}_o$(c)	$E^{\ddagger}_o$(d)	$E^{\ddagger}_c$(a)	$E^{\ddagger}_c$(b)	$E^{\ddagger}_c$(c)	$E^{\ddagger}_c$(d)
MP2/G3MP2Large	148	107	61	179	174	151	115	209
G3(MP2)-RAD	152	111	68	189	180	155	121	217

[a] See Figures 2 and 3 for designation of barriers along the reaction pathways.

3. Results and Discussion

3.1. Choice of Method and Cluster Size. In order to systematically investigate the effect of various chemical modifications on the catalytic properties of the zeolites, we have chosen a wide range of 4T-clusters as our principal substrates (**1**−**15**, Figure 1).

The choice of models is designed to allow an examination of the effect on the energy profile of a variety of alterations in chemical composition with respect to **1**. The model systems do not in all cases represent fragments of presently known zeolites, nor do we advocate all of them to be fragments of feasible or straightforward synthetic targets. Rather, they are intended to facilitate the design of zeolites that are likely to be effective hydrogenation catalysts. The modifications include substitution of the oxygen atoms (**2**−**4**), the acidic proton (**5**−**7**), the framework Al and Si atoms (**8**−**10**), as well as a combination of changes of these types (**11**−**15**).

For the related $HAlX_4$-catalyzed hydrogenation of ethene, we previously found that MP2 with a large basis set yields barriers that are in good agreement with high-level G2 values.[10c] To further assist in choosing a suitable level of theory for examining the systems in the present study, we have carried out preliminary benchmarking calculations for the MP2/G3MP2Large level, against high-level G3(MP2)-RAD[23] values (Table 1).

The results show good accord between the MP2/G3MP2Large and G3(MP2)-RAD barriers and enthalpies, with the former generally slightly lower (mean deviation (MP2 − G3(MP2)-RAD) = −3 kJ mol^{-1}). They also demonstrate the large potential catalytic effect of zeolites for hydrogenation, with the overall barrier being reduced by as much as 240 kJ mol^{-1} (reaction c).

It has previously been found that 4T-clusters similar to those employed in the present study provide an adequate qualitative picture of the local chemical properties in zeolite active sites.[28] To further evaluate the validity of employing these clusters as zeolite models, we have compared the hydrogenation reactions catalyzed by **1**, **2**, and **15** with those catalyzed by their respective larger 28T-clusters (Supporting Information, Table S3). We find that, apart from a few reactions catalyzed by **1** and **1**(28T), the barriers obtained with the 4T-clusters are somewhat lower than those calculated with the 28T-clusters, as reflected in a mean difference of −14 kJ mol^{-1} and a mean absolute difference of 20 kJ mol^{-1} between the two sets of results ($E^{\ddagger}$(4T) − $E^{\ddagger}$(28T),

(24) (a) Flanigen, E. M.; Bennett, J. M.; Grose, R. W.; Cohen, J. P.; Patton, R. L.; Kirchner, R. M.; Smith, J. V. *Nature* **1978**, *271*, 512. (b) Kokotailo, G. T.; Lawton, S. L.; Olson, D. H.; Meier, W. M. *Nature* **1978**, *272*, 437.
(25) The ZSM-5 crystal structure was obtained from the Inorganic Crystal Structure Database (ICSD) and was originally published in Olsen, D. H.; Kokotailo, G. T.; Lawton, S. L.; Meier, W. M. *J. Phys. Chem.* **1981**, *85*, 2238.
(26) See for example:(a) Dapprich, S.; Komiromi, I.; Byun, K. S.; Morokuma, K.; Frisch, M. J. *THEOCHEM* **1999**, *461*−*462*, 1. (b) Vreven, T.; Byun, K. S.; Komaromi, I.; Dapprich, S.; Montgomery, J. A., Jr.; Morokuma, K.; Frisch, M. J. *J. Chem. Theory Comput.* **2006**, *2*, 815.
(27) Scott, A. P.; Radom, L. *J. Phys. Chem.* **1996**, *100*, 16502.
(28) See for example: (a) Kramer, G. J.; de Man, A. J. M.; van Santen, R. A. *J. Am. Chem. Soc.* **1991**, *113*, 6435. (b) Frash, M. V.; van Santen, R. A. *Top. Catal.* **1999**, *9*, 191. (c) Esteves, P. M.; Nascimento, M. A. C.; Mota, C. J. A. *J. Phys. Chem. B* **1999**, *103*, 10417.

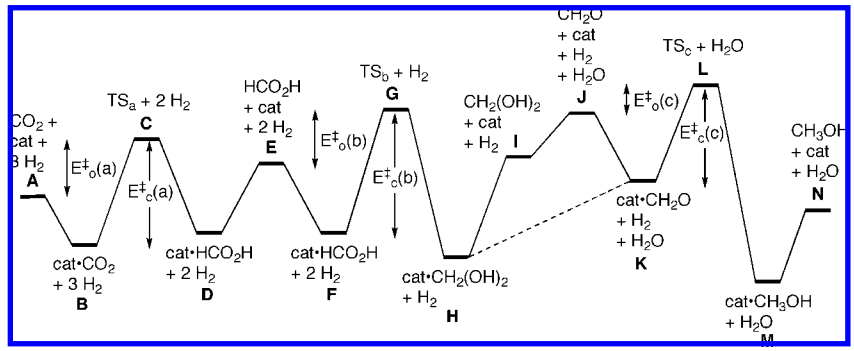

Figure 2. General reaction profile for the three-stage zeolite-catalyzed hydrogenation of CO_2 to give CH_3OH. $E^{\ddagger}_o(x)$ and $E^{\ddagger}_c(x)$ represent overall and central barriers, respectively, for reaction x.

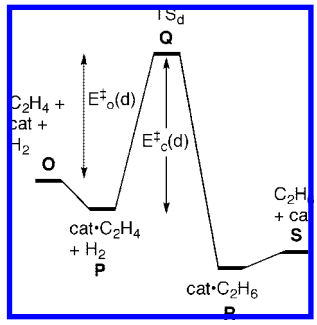

Figure 3. General reaction profile for the zeolite-catalyzed hydrogenation of C_2H_4.

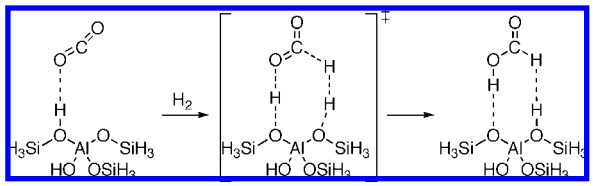

Figure 4. Concerted hydrogenation of CO_2 catalyzed by **1**.

24 comparisons). Nonetheless, the qualitative trends for the 4T-clusters are consistent with those for the 28T-clusters in most cases. Therefore, we have chosen to use the 4T-clusters for our study, expecting at least a good qualitative correspondence.

3.2. General Features of the Catalytic Reactions. We have previously reported preliminary results on the three-stage hydrogenation of CO_2 catalyzed by clusters **1**, **2**, **6**, **10**, and **15**.[17] We found that the three-stage hydrogenation of CO_2 can be described by the general reaction profile shown in Figure 2, where each hydrogenation reaction is characterized by a two-well energy profile. We now find that the zeolite-catalyzed hydrogenation of C_2H_4 also proceeds via such a reaction pathway (Figure 3).

Thus, the substrate initially forms a complex with the zeolite catalyst (e.g., Figure 4). This complex then reacts with H_2, via a concerted transition structure, to form a complex between the product and the catalyst, which can dissociate to give the product and regenerate the catalyst. This type of energy profile has been observed in gas-phase S_N2 reactions,[29] as well as in base-catalyzed hydrogenation reactions.[10f]

We find that the reaction profiles shown in Figures 2 and 3 are a common feature for all the catalytic-hydrogenation reactions investigated in this study. In addition to the concerted pathway, zeolite-catalyzed hydrogenations might also proceed in a stepwise fashion, with the initial formation of a covalently bonded adduct between the substrate and the catalyst, followed by hydrogenolysis of the adduct with H_2. However, a previous investigation on related systems found that the concerted pathway is more favorable,[10d] and we therefore focus on the concerted pathway in the present study.

The optimized structures for **1** and **6** (the sodiated analogue of **1**), and the corresponding complexes and TSs involved in the first step of the catalytic hydrogenation of CO_2, are shown in Figure 5 as representative examples for species involved in all the hydrogenation reactions.[30] The structures for the species containing a reactive H^+ in the catalyst (**1**) are qualitatively different from those containing Na^+ (**6**). In the former case, the H^+ is bonded to one oxygen atom, while in the latter the Na^+ cation assumes a bridging position and is bonded to two oxygen atoms.

The overall barriers ($E^{\ddagger}_o$) and the central barriers ($E^{\ddagger}_c$) for each reaction are given in Table 2.[31] With only a few exceptions, both $E^{\ddagger}_o$ and $E^{\ddagger}_c$ for the hydrogenation of C_2H_4 (reaction d) are higher than those for the corresponding reactions of CO_2 (a), HCO_2H (b), and CH_2O (c). This may in part be attributed to the higher uncatalyzed barrier for reaction d than the barriers for reactions a, b, and c (Supporting Information, Table S3). The presumably more favorable polar interaction between the catalyst and the polar C═O bond in reactions a, b, and c than with the nonpolar C═C bond in reaction d may also contribute to the lower barriers for the reactions of the carbonyls, especially for reactions b and c.

The choice of catalyst affects $E^{\ddagger}_o$ considerably, with the ranges spanned in reactions a, b, c and d being 152, 100, 101, and 124 kJ mol^{-1}, respectively. The variations in $E^{\ddagger}_c$ mostly follow those in $E^{\ddagger}_o$. For instance, changing the catalyst from **1** to **2** leads to an increase in both $E^{\ddagger}_o$(c) (from 60 to 96 kJ mol^{-1}) and $E^{\ddagger}_c$(c) (114 to 125 kJ mol^{-1}) (Table 2).

The ranges spanned by $E^{\ddagger}_c$ are somewhat smaller than those for $E^{\ddagger}_o$, being 126, 68, 51, and 102 kJ mol^{-1} for reactions a, b, c, and d, respectively. The smaller variations in $E^{\ddagger}_c$ can be

(29) For recent reviews on gas-phase S_N2 reactions, see: (a) Chabinyc, M. L.; Craig, S. L.; Regan, C. K.; Brauman, J. I. *Science* **1998**, *279*, 20. (b) Gronert, S. *Chem. Rev.* **2001**, *101*, 329. ((c)) Laerdahl, J. K.; Uggerud, E. *Int. J. Mass Spectrom.* **2002**, *214*, 277. See also: (d) Shaik, S. S.; Schlegel, H. B.; Wolfe, S. *Theoretical Aspects of Physical Organic Chemistry: The S_N2 Mechanism*; Wiley: New York, 1992.

(30) Optimized geometries for the TSs involved in the hydrogenation of HCO_2H, CH_2O, and C_2H_4 (as well as CO_2) catalyzed by **1** and **6** are provided in the Supporting Information (Figure S1).

(31) Energies along the reaction pathway for the zeolite-catalyzed complete hydrogenation of CO_2 to CH_3OH, and for the hydrogenation of C_2H_4, are presented in Tables S4 and S5, respectively, of the Supporting Information.

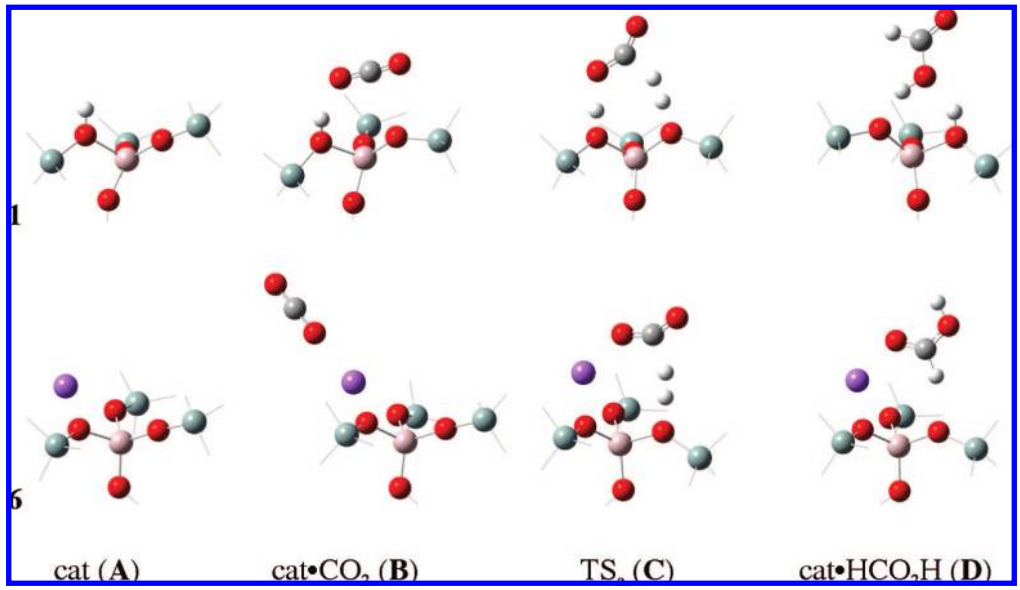

Figure 5. Selected optimized structures for the catalyst-containing components at points **A**, **B**, **C**, and **D** on the reaction potential surface (corresponding to the conversion of carbon dioxide to formic acid, see Figure 1) involving catalyst **1** and its sodiated analogue **6**.

Table 2. Overall ($E^{\ddagger}_{o}$) and Central ($E^{\ddagger}_{c}$) Barriers (kJ mol^{-1}) for Hydrogenation Reactions Catalyzed by Zeolites **1**−**15**[a]

catalyst	$E^{\ddagger}_{o}$(a)	$E^{\ddagger}_{o}$(b)	$E^{\ddagger}_{o}$(c)	$E^{\ddagger}_{o}$(d)	$E^{\ddagger}_{c}$(a)	$E^{\ddagger}_{c}$(b)	$E^{\ddagger}_{c}$(c)	$E^{\ddagger}_{c}$(d)
1	148	107	60	179	174	151	114	209
2	139	134	96	208	162	167	125	223
3	133	49	−5	84	172	111	88	133
4	195	112	65	160	214	135	93	180
5	108	96	54	196	146	179	120	235
6	112	108	66	202	142	183	119	232
7	108	76	35	176	151	170	118	225
8	144	99	56	175	171	148	110	206
9	115	98	55	172	145	157	104	201
10	127	105	61	176	156	158	106	202
11	103	102	64	169	126	134	92	185
12	77	67	29	165	110	150	83	200
13	77	64	29	136	117	143	102	187
14	43	34	3	86	88	112	74	136
15	67	56	17	137	103	120	74	177

[a] See Figure 1 for a display of the zeolite models, and Figures 2 and 3 for the designation of barriers along the reaction pathway.

attributed to the fact that the nature of the interactions between the substrate and the catalyst for the complex are similar to those for the TS, leading to a partial cancelation effect. For example, in the catalytic hydrogenation of CH_2O, both the complexes and the TS involve the CH_2O oxygen interacting with H^+ or M^{n+}, and this in turn leads to similar variations in the complexation energies and $E^{\ddagger}_{o}$. Thus, while $E^{\ddagger}_{o}$(c) increases by 36 kJ mol^{-1} (Table 2) upon substituting catalyst **1** by **2**, the complexation energy increases by 25 kJ mol^{-1} (Table S4, Supporting Information, **1K** versus **2K**), so that $E^{\ddagger}_{c}$(c) only changes by 11 kJ mol^{-1}.

3.3. Substitution of O. Substituting the O atoms in **1** by NH groups (**2**) leads to an $E^{\ddagger}_{o}$(a) that is somewhat lower than that for **1**, while $E^{\ddagger}_{o}$(b), $E^{\ddagger}_{o}$(c), and $E^{\ddagger}_{o}$(d) are considerably higher (by ∼30 kJ mol^{-1}, Table 2). In contrast, the use of **3** (substituting F for $OSiH_3$) gives rise to a lower $E^{\ddagger}_{o}$ for all four hydrogenation reactions. The effects on $E^{\ddagger}_{o}$(b), $E^{\ddagger}_{o}$(c), and $E^{\ddagger}_{o}$(d) (∼60−70 kJ mol^{-1}) are much larger than the effect on $E^{\ddagger}_{o}$(a) (12 kJ mol^{-1}). Going from **1** to **4** (substituting S for O) leads to a considerably higher $E^{\ddagger}_{o}$(a) (by 50 kJ mol^{-1}), while $E^{\ddagger}_{o}$(b) and $E^{\ddagger}_{o}$(c) for **4** are similar to the values for **1**. For reaction d, going from **1** to **4** gives rise to a lower $E^{\ddagger}_{o}$(d) (by 20 kJ mol^{-1}). The observed trends for $E^{\ddagger}_{c}$ generally parallel those for $E^{\ddagger}_{o}$.

Substitution of the O atoms in **1** by NH, F, or S (**2**−**4**) is likely to have a significant effect on the acid/base properties of the catalyst. For example, the acidities of first-row hydrides increases in the order $NH_3 < H_2O < HF$, while the basicities increase in the opposite order: $HF < H_2O < NH_3$.[32] Consequently, one could expect the zeolite catalysts **1**−**3** to become more acidic in the order **2** < **1** < **3**, and the basicities to increase in the opposite order **3** < **1** < **2**. Indeed, the higher basicity for the Si−NH−Si moiety in a zeolite compared with that for Si−O−Si has been previously demonstrated both theoretically and by experiment.[33] It has also been found that HF-doped zeolites are more acidic than standard H-ZSM-5,[8c,34] while Al−NH_2−Si moieties are weaker acids compared with Al−OH−Si.[33a] Catalyst **4**, in which the O atoms in **1** are substituted by S, might be expected to be more acidic and more basic than **1**, as H_2S is both more acidic as well as more basic than H_2O.[35]

As the use of different catalysts has varying effects on reactions a, b, and c, it is probable that these three reactions respond differently toward a change in the acid/base properties of the catalyst. For instance, we find that the use of the more

(32) The experimental gas-phase acidities for NH_3, H_2O, and HF are 1688, 1633, and 1554 kJ mol^{-1}, respectively. Note that a *smaller* value for the acidity corresponds to a *stronger* acid. The experimental gas-phase proton affinities (PA) for HF, H_2O, and NH_3 are 484, 691, and 854 kJ mol^{-1}. A *larger* PA corresponds to a *stronger* base. All experimental acidities and proton affinities are taken from the NIST Chemistry Webbook: Linstrom, P. J.; Mallard, W. G., Eds. *NIST Chemistry WebBook, NIST Standard Reference Database Number 69*; National Institute of Standards and Technology: Gaithersburg, MD, June 2005, http://webbook.nist.gov (accessed January, 2008).

(33) See, for example:(a) Astala, R.; Auerbach, S. M. *J. Am. Chem. Soc.* **2004**, *126*, 1843. (b) Han, A.-J.; He, H.-Y.; Guo, J.; Yu, H.; Huang, Y.-F.; Long, Y.-C. *Microporous Mesoporous Mater.* **2005**, *79*, 177. (c) Elanany, M.; Su, B.-L.; Vercauteren, D. P. *J. Mol. Catal. A* **2007**, *263*, 195.

(34) Le Van Mao, R.; Le, T. S.; Fairbairn, M.; Muntasar, A.; Xiao, S.; Denes, G. *Appl. Catal., A* **1999**, *185*, 41.

(35) The gas-phase acidity for H_2S is 1468−1473 kJ mol^{-1} (cf. 1633 kJ mol^{-1} for H_2O) while its PA is 705 kJ mol^{-1} (cf. 691 kJ mol^{-1} for H_2O).

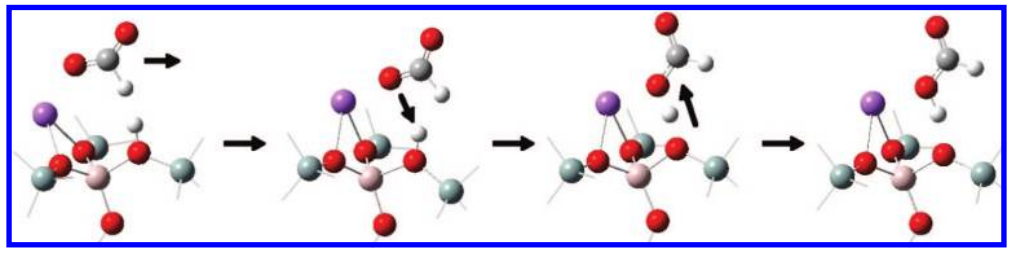

Figure 6. Spontaneous rearrangement of the product complex from the **6**-catalyzed hydrogenation of CO_2 to regenerate the active catalyst.

acidic catalyst **3**, when compared with **1**, leads to a substantially lower barrier for reaction d. For reaction a, both **2** and **3** lead to a somewhat lower $E^{\ddagger}_o$, and this might indicate the importance of both the acidity and basicity of the catalyst for this reaction. On the other hand, the higher $E^{\ddagger}_o$(b), $E^{\ddagger}_o$(c), and $E^{\ddagger}_o$(d) for **2**, and the lower corresponding values for **3**, might suggest that for these three reactions the acidity of the catalyst influences their $E^{\ddagger}_o$ more than the basicity. Despite catalyst **4** being expected to be more acidic *and* more basic than **1**, it leads to higher $E^{\ddagger}_o$ values for reactions a, b, and c. This indicates the presence of factors other than acidity and basicity of the catalyst in these catalytic processes. On the other hand, **4**, when compared with **1**, leads to a lower $E^{\ddagger}_o$(d) as opposed to higher $E^{\ddagger}_o$ values for reactions a, b, and c. This finding is consistent with previous observations on the acid-catalyzed hydrogenation of ethene,[10e] in which H_2S is found to be a better catalyst than H_2O, and indicates different requirements in the catalytic hydrogenation of a nonpolar C=C bond versus a polar C=O bond.

3.4. Substitution of H^+. In principle, reactions that involve a metal-cation-containing catalyst (e.g., **6**) are more complicated than protic catalysts, in that they formally give an anion (i.e., HCO_2^-, $CH_2(OH)O^-$, or CH_3O^-) and the protonated catalyst as products, i.e., the catalyst itself appears not to be regenerated. However, we find that optimization of product complexes between protonated-**6** and HCO_2^- (or $CH_2(OH)O^-$ or CH_3O^-) leads to spontaneous rearrangement and proton transfer to give the neutral products (e.g., Figure 6).[36] Hence, it is likely that there is little or no barrier to the regeneration of the active catalyst. This leads to reaction profiles for reactions catalyzed by metal-cation-containing catalysts that are similar to those depicted in Figures 2 and 3.

Replacing the H^+ in **1** by Li^+ (**5**) leads to lower $E^{\ddagger}_o$ values for the catalytic hydrogenation reactions of CO_2, HCO_2H, and CH_2O (Table 2). The effect is somewhat larger for reaction a (37 kJ mol^{-1}) than for reactions b and c (~10 kJ mol^{-1}). In contrast, when the metal cation is Na^+ (**6**), while $E^{\ddagger}_o$(a) is 33 kJ mol^{-1} lower than that for **1**, $E^{\ddagger}_o$(b) and $E^{\ddagger}_o$(c) are somewhat higher than the corresponding values for **1**. Substituting H^+ with $MgOH^+$ (**7**) decreases $E^{\ddagger}_o$ for these three reactions by ~30 kJ mol^{-1}. In contrast, for the reaction of C_2H_4, substitution of H^+ by any metal cation leads to a somewhat higher barrier (by up to ~20 kJ mol^{-1}). Observation of contrasting effects of these substitutions for reactions a, b, and c versus d again demonstrates that the governing factors in zeolite-catalyzed hydrogenation may vary in their importance, depending on the nature of the substrate.

For all four reactions, the $E^{\ddagger}_o$ values for **6** (Na^+) are somewhat higher than those for **5** (Li^+), whereas the $E^{\ddagger}_o$ values for **7** ($MgOH^+$) are all lower than those for **6**. We have previously found that in base-catalyzed hydrogenation, the overall gas-phase barriers increase with respect to the metal cation in the catalyst in the order $Li^+ < Na^+ < K^+$, while alkaline-earth cations are more active than the corresponding alkali metal cations in the same row.[10f] Our observations here are consistent with these previous results and, in a similar way, can be rationalized by considering the differences in charge density on the metal cations. Thus, Na^+ is larger than Li^+ and has a smaller charge density, hence the lower activity and higher $E^{\ddagger}_o$. On the other hand, the higher charge on Mg^{2+} than Na^+ leads to a lower $E^{\ddagger}_o$. While there are considerable variations in $E^{\ddagger}_o$ with respect to the metal cation, the values of $E^{\ddagger}_c$ are comparable for each hydrogenation reaction. This indicates that the interactions between the substrate and the catalyst are very similar in the complexes and in the TS. This is again consistent with our previous observations in base-catalyzed hydrogenation reactions.[10f]

3.5. Substitution of Al and Si. Substituting the Al atom in **1** by Ga (**8**) gives $E^{\ddagger}_o$ and $E^{\ddagger}_c$ values that are very similar to those for **1** for all the reactions (Table 2). On the other hand, while substitution of the Si atoms with C (**9**) or Ge (**10**) does not lead to large changes in $E^{\ddagger}_o$(b) and $E^{\ddagger}_o$(c), the $E^{\ddagger}_o$(a) values for **9** and **10** are considerably smaller than that for **1**. The difference in $E^{\ddagger}_o$(a) is larger for **9** versus **1** (30 kJ mol^{-1}) than for **10** versus **1** (18 kJ mol^{-1}). Similarly, the $E^{\ddagger}_c$(a) values for **9** and **10** are lower than that for **1** by 29 and 18 kJ mol^{-1}, respectively, while their $E^{\ddagger}_c$(b) and $E^{\ddagger}_c$(c) values are comparable to those for **1**. For the hydrogenation of C_2H_4, the use of catalysts **8**−**10** leads to similar $E^{\ddagger}_o$ and $E^{\ddagger}_c$ values when compared with those for **1**.

To rationalize the variations in $E^{\ddagger}_o$ for **1**, **9**, and **10**, the hydrogenation reactions catalyzed by model systems **16**−**18**, and **19**−**21** were studied (Table 3). Catalysts **16**−**18** share a common basic group SiH_3O. Consequently, the dependence of the overall barrier ($E^{\ddagger}_o$) on different acidic groups, namely $HOSiH_3$, $HOCH_3$ and $HOGeH_3$, can be determined. The rationale for choosing SiH_3O as the common basic group is that this moiety is relatively less basic than alternatives (e.g., CH_3O, SiH_3NH). Hence, the effect of different acidic groups can be observed without being overshadowed by the effect of the common basic moiety. Likewise, the impacts of different basic groups (SiH_3O, CH_3O, and GeH_3O) on $E^{\ddagger}_o$ are evaluated using **19**−**21**, which share a common, relatively less acidic moiety NH_2SiH_3.

For the reactions catalyzed by **16**−**18**, the $E^{\ddagger}_o$(a) values do not vary to a large extent, suggesting that the acidity of the catalyst may play only a minor role in the hydrogenation of CO_2. However, $E^{\ddagger}_o$(b), $E^{\ddagger}_o$(c), and $E^{\ddagger}_o$(d) for **16** are lower than the corresponding values for **17** and **18** by more than 10 kJ mol^{-1}, indicating that $HOSiH_3$ is more reactive than both $HOCH_3$ and $HOGeH_3$ for the hydrogenation of HCO_2H, CH_2O,

(36) This pathway was found by taking the last points in the IRC calculations as initial geometries.

Table 3. Overall Barriers ($E^{\ddagger}_{o}$) for Hydrogenation Reactions Catalyzed by **16**−**18**, Which Share a Common Basic Moiety (SiH_3O), and by **19**−**21**, Which Share a Common Acidic Group (NH_2SiH_3)[a]

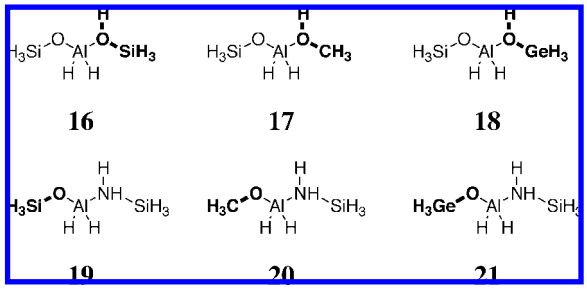

16 **17** **18**

19 **20** **21**

catalyst	$E^{\ddagger}_{o}$(a)	$E^{\ddagger}_{o}$(b)	$E^{\ddagger}_{o}$(c)	$E^{\ddagger}_{o}$(d)
16	146	108	62	176
17	150	127	80	191
18	149	124	77	188
19	171	167	120	232
20	135	132	89	203
21	144	141	100	213

[a] See Figures 2 and 3 for the designation of barriers along the reaction pathway.

and C_2H_4. Turning our attention to **19**−**21** and the effect of the basic moiety, we find that the $E^{\ddagger}_{o}$ values for **19** are substantially higher than those for **21** (by ∼20−30 kJ mol^{-1}), which are in turn somewhat higher than those for **20**. Thus, the SiH_3O moiety is less reactive than both CH_3O and GeH_3O for all four hydrogenation reactions.

The catalyst **1** contains the acidic $HOSiH_3$ group and the basic SiH_3O group, whereas **9** contains $HOCH_3$ and CH_3O, and **10** contains $HOGeH_3$ and GeH_3O. For the hydrogenation of HCO_2H, CH_2O, and C_2H_4 catalyzed by **1**, the relatively low activity of the SiH_3O group, compared with the C and Ge analogues, appears to be offset by the relatively high activity of its $HOSiH_3$ group, leading to comparable $E^{\ddagger}_{o}$(b), $E^{\ddagger}_{o}$(c), and $E^{\ddagger}_{o}$(d) values for catalysts **1**, **9**, and **10**. However, for the hydrogenation of CO_2, the low activity of the SiH_3O moiety in **1** is not offset by the activity of the $HOSiH_3$ group, because it is not significantly different to those of the C and Ge analogues for this reaction (Table 2). As a consequence, $E^{\ddagger}_{o}$(a) for **1** is considerably higher than corresponding values for **9** and **10**. It is also noteworthy that **16** is a simplified model of **1**, in which the OH and the nonparticipating $OSiH_3$ groups in **1** are substituted by H. The fact that the $E^{\ddagger}_{o}$ values for **16** are similar to those for **1** (Table 2) indicates that these nonparticipating moieties do not have a profound influence on the barriers for these hydrogenation reactions.

3.6. Combination of Compositional Variations. In many cases, compositional modifications to **1** lead to a decrease in $E^{\ddagger}_{o}$ and $E^{\ddagger}_{c}$ values which, in some instances, are quite substantial. How would the barriers for the hydrogenation reactions be affected when a catalyst that incorporates two or more favorable compositional changes is used? Ideally, the catalyst would combine the strengths of individual modifications and lead to an even lower $E^{\ddagger}_{o}$. In our previous communication,[17] we demonstrated with **15** that it is even possible to achieve higher catalytic activity than would be expected from a combination of individual features! To explore the fundamentals and exploit the potential of this synergistic effect, catalytic hydrogenation reactions with catalysts **11**−**14** were investigated. These catalysts feature two or three compositional changes with respect to **1** that include a combination of substitution of O with N (**11**, **13**, **14**), H^+ with Li^+ (**12**, **13**, **14**), and Si with C (**11**, **12**, **14**). The rationale for the choice of these chemical modifications, namely the incorporation of N, Li^+, and C, is that these features seem to have a large and, in many cases, favorable individual impact on the barrier.

With only a few exceptions, the $E^{\ddagger}_{o}$ values for **11**−**14** are substantially lower than those for **1** (Table 2). The lowest $E^{\ddagger}_{o}$ values are those for the reactions catalyzed by **14**, which incorporates all three compositional changes. Comparable trends are also observed for $E^{\ddagger}_{c}$ for all four hydrogenation reactions.

To rationalize the variations in $E^{\ddagger}_{o}$ for these "hybrid" catalysts **11**−**14**, the hydrogenation reactions catalyzed by **16**, **19**, **17**, and **22**−**26**, and **19**, **27**, **20**, and **28**, have been investigated. The former group of catalysts share a common basic moiety SiH_3O, whereas the latter have the same acidic group NH_2SiH_3. The results are shown in Tables 4 and 5, respectively, for the two groups.

For reactions catalyzed by **16**, **19**, **17**, and **22**, there are considerable variations in $E^{\ddagger}_{o}$ for all four hydrogenation reactions. The variations in $E^{\ddagger}_{o}$(b), $E^{\ddagger}_{o}$(c), and $E^{\ddagger}_{o}$(d) are larger than those in $E^{\ddagger}_{o}$(a), supporting the hypothesis that the acidity of the reactive XH proton is more important in the hydrogenation reactions of HCO_2H, CH_2O, and C_2H_4 than in the hydrogenation of CO_2.

Catalysts with a reactive NH_2 proton (**19**, **22**) give rise to a considerably higher $E^{\ddagger}_{o}$ than the corresponding catalysts with an OH proton (**16**, **17**). This is consistent with the generally lower acidity of an NH_2 proton than an OH proton. In addition, $E^{\ddagger}_{o}$ values for catalysts with an $HXCH_3$ group (**17**, **22**) are somewhat higher than those with an $HXSiH_3$ group (**16**, **19**).

Reactions a, b, and c generally have lower $E^{\ddagger}_{o}$ values when catalyzed by **23**−**26** than by **16**, **19**, **17**, and **22** (Table 4), indicating that Li^+ is more effective than H^+ for these hydrogenation reactions. The differences in $E^{\ddagger}_{o}$ between reactions that are catalyzed by H^+-based catalysts and by Li^+-based catalysts are generally larger for the hydrogenation of CO_2 ($E^{\ddagger}_{o}$(a)) than for hydrogenation of HCO_2H ($E^{\ddagger}_{o}$(b)) and CH_2O ($E^{\ddagger}_{o}$(c)). On the other hand, substituting H^+ by a Li^+ can lead to a higher barrier for the hydrogenation of C_2H_4. In contrast to reactions involving H^+-based catalysts, the use of a variety of Li^+-based catalysts leads to only a small variation in $E^{\ddagger}_{o}$ (<10 kJ mol^{-1} for **23**−**26**). Thus, the activity of these catalysts, in which the Li^+ ion serves the purpose of activating the substrate, is relatively insensitive to the X group attached to Li^+. It is also noteworthy that catalyst **23** and catalyst **5** differ only by a substituent on Al, i.e., an OH for **23** and an H for **5**. The similarities in their $E^{\ddagger}_{o}$ values (Tables 2 and 4) further supports the view that the catalytic activity of the zeolite is relatively insensitive to the nature of nonparticipating substituents on Al.

For the reactions catalyzed by **19**, **27**, **20**, and **28** (Table 5), there are considerable variations in $E^{\ddagger}_{o}$ for all four reactions. The ranges in $E^{\ddagger}_{o}$(a), $E^{\ddagger}_{o}$(b), $E^{\ddagger}_{o}$(c), and $E^{\ddagger}_{o}$(d) are comparable. This suggests that the basicities of the basic moiety in the catalysts are of similar importance in the hydrogenation reactions of CO_2, HCO_2H, CH_2O, and C_2H_4. The $E^{\ddagger}_{o}$ values for catalysts with an N-base (**27**, **28**) are significantly smaller than those with an O-base (**19**, **27**). This is consistent with the higher basicity of an N-base than an O-base. Furthermore, catalysts with a CH_3X group (**20**, **28**) give rise to lower $E^{\ddagger}_{o}$ values than the corresponding catalysts with an SiH_3X group (**19**, **27**).

The above results illustrate the effect on $E^{\ddagger}_{o}$ of changing either the acidic or the basic group. We now examine the effect of

Table 4. Overall Barriers for Hydrogenation Reactions Catalyzed by **16**, **19**, **17** and **22**, and **23**−**26**, Which Share a Common Basic Group (SiH_3O)[a,b]

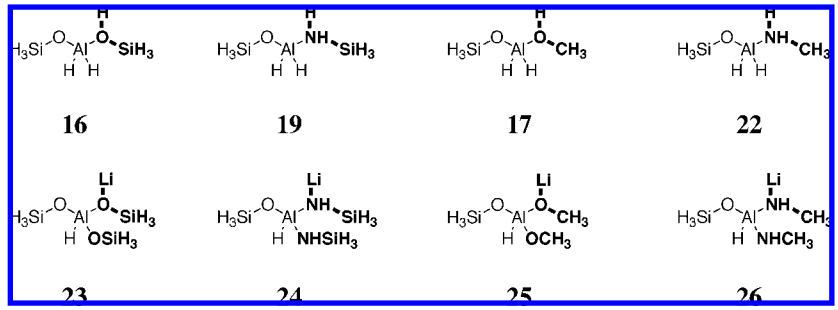

catalyst	$E^{\ddagger}_o$(a)	$E^{\ddagger}_o$(b)	$E^{\ddagger}_o$(c)	$E^{\ddagger}_o$(d)
16	146 (0)	108 (0)	62 (0)	176 (0)
19	171 (25)	167 (59)	120 (58)	232 (56)
17	150 (4)	127 (19)	80 (18)	192 (16)
22	172 (26)	170 (62)	125 (63)	241 (65)
23	110 (−36)	98 (−10)	56 (−6)	198 (22)
24	113 (−33)	102 (−6)	60 (−2)	202 (26)
25	114 (−32)	107 (−1)	66 (4)	206 (30)
26	111 (−35)	105 (−3)	64 (2)	195 (19)

[a] See Figures 2 and 3 for designation of barriers along the reaction pathway. [b] The differences in $E^{\ddagger}_o$ values relative to those for **16** are given in parentheses.

Table 5. Overall Barriers for Hydrogenation Reactions Catalyzed by **19**, **27**, **20**, and **28**, Which Share a Common Acidic Moiety (NH_2SiH_3)[a,b]

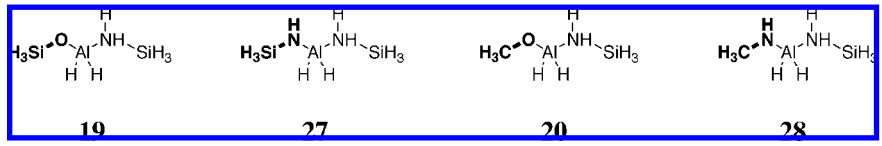

catalyst	$E^{\ddagger}_o$(a)	$E^{\ddagger}_o$(b)	$E^{\ddagger}_o$(c)	$E^{\ddagger}_o$(d)
19	171 (0)	167 (0)	120 (0)	232 (0)
27	142 (−29)	138 (−29)	96 (−24)	205 (−27)
20	135 (−36)	132 (−35)	89 (−31)	203 (−29)
28	109 (−62)	105 (−62)	68 (−52)	173 (−59)

[a] See Figures 2 and 3 for designation of barriers along the reaction pathway. [b] The differences in $E^{\ddagger}_o$ values relative to those for **19** are given in parentheses.

modifying both the acidic group and the basic group simultaneously. Considering catalysts **1** and **2**, the compositional changes that might be expected to have the greatest impact on the catalytic activity are those related to the participating acidic group ($HOSiH_3 \rightarrow NH_2SiH_3$) and the participating basic group ($SiH_3O \rightarrow SiH_3NH$). These are the same as the differences between **16** and **19**, and between **19** and **27**, respectively. Consequently, one might expect the differences in $E^{\ddagger}_o$ for **1** and **2** to correlate with the differences in $E^{\ddagger}_o$ between **16** and **19**, and between **19** and **27**.

On the basis of this concept, we have "estimated" $E^{\ddagger}_o$ for some selected reactions using an additivity scheme. In this scheme, to obtain the estimated $E^{\ddagger}_o$(a) for catalyst **2**, the $E^{\ddagger}_o$(a) for **1** (148 kJ mol^{-1}) is used as the base value. To this base value the sum of differences in $E^{\ddagger}_o$(a) ($\sum \Delta E^{\ddagger}_o$(a)) that correspond to the relevant compositional changes ($E^{\ddagger}_o$(a,**19**) − $E^{\ddagger}_o$(a,**16**) = +25 kJ mol^{-1} and $E^{\ddagger}_o$(a,**27**) − $E^{\ddagger}_o$(a,**19**) = −29 kJ mol^{-1}) are added to give the estimated value for $E^{\ddagger}_o$(a) (148 + (+25 + −29) = 144 kJ mol^{-1}). For all estimated $E^{\ddagger}_o$, the $E^{\ddagger}_o$ values for catalyst **1** are used as the base values. In addition, the $\Delta E^{\ddagger}_o$ values are calculated with respect to $E^{\ddagger}_o$(**16**) for evaluating the effect of changing the acidic group in the catalyst, or $E^{\ddagger}_o$(**19**) for estimating the effect of altering the basic moiety. The results are summarized in Table 6. The explicitly calculated $E^{\ddagger}_o$ values (Table 2) are included for comparison.

Table 6. Comparison of $E^{\ddagger}_o$ Values Estimated through Additivity with Explicitly Calculated Values for Selected Hydrogenation Reactions[a,b]

	$E^{\ddagger}_o$ estimated[c]			
catalyst[d]	$E^{\ddagger}_o$(a)	$E^{\ddagger}_o$(b)	$E^{\ddagger}_o$(c)	$E^{\ddagger}_o$(d)
2 (**19**, **27**)	144 (139)	137 (134)	95 (96)	208 (208)
5 (**23**, **19**)	112 (108)	97 (96)	55 (54)	201 (196)
9 (**17**, **20**)	116 (115)	91 (98)	47 (55)	166 (172)
11 (**22**, **28**)	112 (103)	107 (102)	72 (64)	185 (169)
12 (**25**, **20**)	80 (77)	71 (64)	34 (29)	180 (165)
13 (**24**, **27**)	86 (77)	72 (67)	35 (29)	178 (136)
14 (**26**, **28**)	51 (43)	42 (34)	11 (3)	139 (86)

[a] See Figures 2 and 3 for designation of barriers along the reaction pathway. [b] The explicitly calculated $E^{\ddagger}_o$ values (Table 2) are given in parentheses alongside the $E^{\ddagger}_o$ values estimated through additivity. [c] $E^{\ddagger}_o$ estimated = $E^{\ddagger}_o$(**1**) + $\sum \Delta E^{\ddagger}_o$. For example, estimated $E^{\ddagger}_o$(a,**2**) = $E^{\ddagger}_o$(a,**1**) + (($E^{\ddagger}_o$(a,**19**) - $E^{\ddagger}_o$(a,**16**)) + ($E^{\ddagger}_o$(a,**27**) - $E^{\ddagger}_o$(a,**19**))). [d] The major compositional changes between a given catalyst and **1** are represented by the catalysts (relative to **16** and **19**, respectively) in parentheses.

There is generally good agreement between the estimated $E^{\ddagger}_o$ and the actual values (±10 kJ mol^{-1}) for reactions a, b, and c. The good performance of this simple additivity scheme indicates that, during the hydrogenation of CO_2, HCO_2H, and CH_2O, there is little in the way of synergistic interaction between the active acidic and basic groups. In other words, activation of the

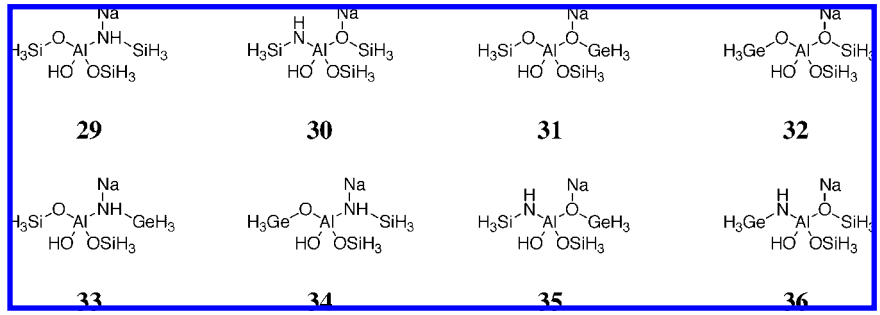

Figure 7. Models that represent local active sites in an alkali metal (Na^+) zeolite with partial substitution of Si by Ge and O by NH.

substrate by the acidic moiety and the activation of H_2 by the basic moiety are rather independent of one another. On the other hand, there exist larger differences between the estimated and explicitly calculated barriers for the hydrogenation of C_2H_4, particularly for those reactions catalyzed by **11**−**14**. In these cases, the actual barriers are substantially lower than the values estimated by additivity (by up to ∼50 kJ mol^{-1}). This points toward the existence of synergistic interactions between the acidic and basic groups for the zeolite-catalyzed hydrogenation of C_2H_4 and further demonstrates the difference between polar and nonpolar substrates in their zeolite-catalyzed hydrogenations.

3.7. Design of an Effective Zeolite. Given the insights gained from the previous sections, can we design a zeolite that possesses good catalytic activity for hydrogenation reactions? The catalyst should have high acidity for activating the substrate, as well as high basicity to assist the heterolytic cleavage of H_2. As the basicity of an X group increases, the corresponding XH moiety generally becomes less acidic, i.e., leads to a less favorable contribution, i.e., the two effects work against one another. However, if the acidic proton is replaced by an alkali metal cation, i.e., XM, its catalytic activity does not significantly decrease as X becomes more basic. Thus, a good zeolite for catalyzing hydrogenation would ideally be quite basic and have the reactive acidic protons replaced by alkali metal cations.

Compound **14** satisfies the above conditions and is theoretically the most active among the range of catalysts examined (Table 2). However, the immediate application of a zeolite based on **14** might be difficult, as, to the best of our knowledge, a zeolite with Si atoms substituted by C is unknown. On the other hand, although a GeH_3O moiety is less active than CH_3O, it is considerably more active than SiH_3O (Table 3). The synthesis of zeolites that have Si atoms substituted by Ge is comparatively more straightforward,[16c,37] though we are aware that Ge-based frameworks may sometimes have stability issues.[38] In addition, zeolites with framework O atoms replaced by N have also been synthesized.[13] Although **14** contains Li^+ as the alkali metal cation, the use of Na^+ instead of Li^+ seems to be an appropriate choice, as the catalytic activities of the two cations are comparable (Table 2), and Na^+ is more commonly used experimentally. Thus, a zeolite based on **15** is deemed an appropriate synthetic target in terms of achieving a balance between catalytic activity and synthetic feasibility.[39]

3.8. Partial Substitutions. As the full substitution of Si with Ge and O with NH is not trivial experimentally, we have evaluated the catalytic activity of partially substituted zeolites based on **15**. Thus, the hydrogenation reactions catalyzed by **29**−**36** have been examined (Figure 7).[40] These models represent some of the possible local active structures in an alkali metal zeolite that partially incorporates Ge, N, and Na^+. Note that the pairs **29** and **30**, and **31** and **32**, and the quartet **33**−**36**, are isomeric.

The energies of **29** and **30** are comparable, with **30** lying 1 kJ mol^{-1} higher than **29**. Similarly, the energy of **32** lies 6 kJ mol^{-1} higher than that of **31**. On the other hand, the variations in the energies of **33**−**36** are larger. While **36** lies only 3 kJ mol^{-1} higher in energy than **33**, the energies of **34** and **35** are 29 and 43 kJ mol^{-1}, respectively, higher than that of **33**. Our calculated relative energies of **33**−**36** indicate that, in a zeolite that incorporates both Ge and N, it is likely to find an N atom adjacent to a Ge atom (**33** and **36**).

The overall and central barriers for the hydrogenation reactions catalyzed by **29**−**36** are summarized in Table 7. For all four hydrogenation reactions, the values of $E^{\ddagger}_o$ and $E^{\ddagger}_c$ vary over a range of approximately 40−60 kJ mol^{-1}, with the lowest $E^{\ddagger}_o$ and $E^{\ddagger}_c$ values being somewhat higher than those for **15** (Table 2). As mentioned above, among the isomeric models **33**−**36**, one of the more stable isomers is **36**. Importantly, while there are wide ranges of overall and central barriers for **33**−**36**, the barriers for **36** are among the lowest. Thus, for a zeolite that incorporates Ge and N, with a variable degree of substitution, one could expect a fair catalytic activity for hydrogenation.

(37) See, for example: (a) van de Water, L. G. A.; van der Waal, J. C.; Jansen, J. C.; Cadoni, M.; Marchese, L.; Maschmeyer, T. *J. Phys. Chem. B* **2003**, *107*, 10423. (b) van de Water, L. G. A.; Zwijnenburg, M. A.; Sloof, W. G.; van der Waal, J. C.; Jansen, J. C.; Maschmeyer, T. *ChemPhysChem* **2004**, *5*, 1328. (c) Cheng, C. H.; Juttu, G.; Mitchell, S. F.; Shantz, D. F. *J. Phys. Chem. B* **2006**, *110*, 22488.

(38) (a) Li, Q.; Navrotsky, A.; Rey, F.; Corma, A. *Microporous Mesoporous Mater.* **2003**, *64*, 127. (b) Sastre, G.; Pulido, A.; Corma, A. *Microporous Mesoporous Mater.* **2005**, *82*, 159.

(39) We have also examined Li and MgOH analogues of **15** (Na). The former has $E^{\ddagger}_o$ values for reactions a, b, c, and d of 55, 45, 9, and 128 kJ mol^{-1}, respectively, with the corresponding $E^{\ddagger}_c$ values of 88, 113, 65, and 165 kJ mol^{-1}, while the latter has $E^{\ddagger}_o$ values for reactions a, b, c, and d of 62, 35,−3, and 134 kJ mol^{-1}, respectively, with corresponding $E^{\ddagger}_c$ values of 115, 125, 121, and 165 kJ mol^{-1}. The $E^{\ddagger}_o$ and $E^{\ddagger}_c$ values for the Li and MgOH analogues are thus generally slightly better than those for **15** ($E^{\ddagger}_o$ for reactions a, b, c, and d = 67, 56, 17, and 137 kJ mol^{-1}, respectively, and $E^{\ddagger}_c$ for reactions a, b, c, and d = 103, 120, 74, and 177 kJ mol^{-1}, respectively, Table 2).

(40) We have also carried out preliminary calculations on several 8T-clusters (Table S7, Supporting Information). Each 8T-cluster contains an Al, Ge, N, and Na atom. The results indicate that in a zeolite that incorporates these modifications, it is likely to have NH−Ge moieties within the framework. It has also been found that in a Ge-containing zeolite, it is not necessary for the Ge atom to be directly adjacent to the AlOH center in order to have a large effect on the strength of the acidic site (ref 37b).

Table 7. Overall ($E^{\ddagger}_o$) and Central ($E^{\ddagger}_c$) Barriers (kJ mol^{-1}) for Hydrogenation Reactions Catalyzed by **29**−**36**, Which Represent Local Active Site Structures for an Alkali Metal (Na^+) Zeolite That Partially Incorporates Ge and N[a]

catalyst	$E^{\ddagger}_o$(a)	$E^{\ddagger}_o$(b)	$E^{\ddagger}_o$(c)	$E^{\ddagger}_o$(d)	$E^{\ddagger}_c$(a)	$E^{\ddagger}_c$(b)	$E^{\ddagger}_c$(c)	$E^{\ddagger}_c$(d)
29	126	123	81	216	153	183	135	237
30	94	88	51	166	121	147	106	199
31	106	103	61	198	148	181	132	235
32	84	78	39	171	131	160	114	212
33	134	130	90	218	157	180	134	241
34	105	101	61	190	130	160	113	219
35	79	73	36	151	117	145	104	196
36	76	76	40	146	99	137	94	180

[a] See Figures 2 and 3 for designation of barriers along the reaction pathway.

4. Concluding Remarks

Ab initio molecular orbital theory and density functional theory calculations have been applied to the study of the three-stage zeolite-catalyzed hydrogenation of CO_2 to methanol, and the zeolite-catalyzed hydrogenation of C_2H_4 to ethane. The following important points emerge from the present study:

1. Zeolites provide effective catalysis for the complete hydrogenation of CO_2 to CH_3OH and for the hydrogenation of C_2H_4 to ethane, with a substantial lowering of the reaction barrier (by more than 200 kJ mol^{-1}) compared with the uncatalyzed reactions. We find that the zeolites are generally better catalysts for the hydrogenation of CO_2, HCO_2H, and CH_2O than for C_2H_4. However, **3** ($HAlF_4$) and **14** ($CH_3-O-Al(OH)(OCH_3)-OLi-OCH_3$) are found to be particularly effective catalysts for the hydrogenation of C_2H_4.

2. The zeolite-catalyzed hydrogenation reactions of CO_2, HCO_2H, and CH_2O are sensitive to both the acidity of the XH moiety or the nature of the metal cation (M) in the XM moiety, and the basicity of the adjacent X group in the catalyst (-X−Al−XH- or -X−Al−XM-). In general, a more acidic XH, an M with a higher charge density, or a more basic X leads to a lowering of the barrier for the reaction.

3. Hydrogenation reactions of HCO_2H and CH_2O are more sensitive to the acidity of the active proton of the catalyst than the reaction of CO_2, while all three reactions show a similar dependence on the basicity of the X group. The zeolite that contains second-row SH and S groups is a better catalyst than the corresponding oxygen analogue for the hydrogenation of C_2H_4 but less effective for the hydrogenation of CO_2, HCO_2H, and CH_2O.

4. For the hydrogenation of CO_2, HCO_2H, and CH_2O, the barriers can be estimated by considering contributions from the acidic XH or the XM moiety and the basic X moiety independently. However, for the hydrogenation of C_2H_4, the synergistic combination of the acidic and basic groups of the catalyst leads to lower barriers than would be predicted by considering the two moieties independently.

5. For protic zeolites, compositional variations that give rise to a more acidic XH generally lower the basicity of X. Thus, the variation in reaction barriers depends not only on the catalyst but also on the sensitivity of the reaction to acidity/basicity, i.e., the nature of the substrate. When an alkali metal cation is used instead of H^+, the catalytic activity of the cation is less sensitive to the nature of the underlying ligands X in the XM moiety, even when there is a large variation in the basicity of X. Consequently, the reactivity of an alkali metal zeolite increases as X becomes more basic.

6. An effective zeolite for the hydrogenation of CO_2, HCO_2H, and CH_2O should in the first instance be a reasonably basic alkali metal zeolite. We propose that a zeolite with Ge, N, and Na^+ incorporated into the framework would represent an appropriate balance between the catalytic activity and the practical ease of synthesis and usage.

Acknowledgment. We gratefully acknowledge generous allocations of computing time from the National Facility of the Australian Partnership for Advanced Computing (APAC) and the Australian Center for Advanced Computing and Communications (ac3), the provision (to B.C.) of a New Zealand Science & Technology Postdoctoral Fellowship by the Foundation for Research, Science & Technology, and funding (to L.R.) from an Australian Research Council Discovery Grant and from the ARC Centre of Excellence for Free Radical Chemistry and Biotechnology.

Supporting Information Available: GAUSSIAN 03 archive entries for B3-LYP/6−31+G(d,p)- and ONIOM(B3-LYP/6−31+G(d,p):PM3)-optimized geometries of relevant equilibrium structures and transition structures (Table S1), calculated MP2/G3MP2Large and ONIOM(MP2/G3MP2Large:HF/6−31+G(d,p)) total energies (Table S2), MP2/G3MP2Large barriers for the reactions a−d catalyzed by **1**, **2**, and **15** and ONIOM(MP2/G3MP2Large:HF/6−31+G(d,p)) barriers for the corresponding 28T-clusters (Table S3), MP2/G3MP2Large relative energies along the reaction pathway for reactions a−d catalyzed by **1**−**15** (Tables S4 and S5), selected bond lengths for transition structures involving **1**−**15** (Table S6), MP2/G3MP2Large relative energies for isomeric 8T-clusters (Table S7), geometries for the TSs for reactions a−d catalyzed by **1** and **6** (Figure S1), and full citations for references 1a, 20, and 21. This material is available free of charge via the Internet at http://pubs.acs.org.

JA800840Q